A Journal of the Gesellschaft Deutscher Chemiker

Angewandte International Edition GDCh Chemie

www.angewandte.org

Accepted Article

Title: In situ assembly of choline acetyltransferase ligands by a hydrothiolation reaction reveals key determinants for inhibitor design

Authors: Daniel Wiktelius, Anders Allgardsson, Tomas Bergström, Norman Hoster, Christine Akfur, Nina Forsgren, Christian Lejon, Mattias Hedenström, Anna Linusson, and Fredrik Ekström

To be cited as: *Angew. Chem. Int. Ed.* 10.1002/anie.202011989

Link to VoR: https://doi.org/10.1002/anie.202011989

WILEY-VCH

10.1002/anie.202011989

WILEY-VCH

RESEARCH ARTICLE

In situ assembly of choline acetyltransferase ligands by a hydrothiolation reaction reveals key determinants for inhibitor design

Daniel Wiktelius[+], Anders Allgardsson[+], Tomas Bergström, Norman Hoster, Christine Akfur, Nina Forsgren, Christian Lejon, Mattias Hedenström, Anna Linusson and Fredrik Ekström*

[*] Dr. D. Wiktelius[+], Dr. A. Allgardsson[+], Dr. Tomas Bergström, B.Sc. C. Akfur, Dr. N. Forsgren, MSc. C. Lejon, Dr. F. Ekström
Swedish Defence Research Agency
CBRN Defence and Security
SE-901 82 (Sweden)
E-mail: fredrik.ekstrom@foi.se
M.Sc. N. Hoster, Dr. Mattias Hedenström, Prof. Dr. Anna Linusson
Department of Chemistry, Umeå University
901 87 Umeå (Sweden)

+ These authors contributed equally to this work

Supporting information for this article is given via a link at the end of the document.

Abstract: The potential drug target choline acetyltransferase (ChAT) catalyzes the production of the neurotransmitter acetylcholine in cholinergic neurons, T-cells, and B-cells. Herein, we show that arylvinylpyridiniums (AVPs), the most widely studied class of ChAT inhibitors, act as substrate in an unusual coenzyme A-dependent hydrothiolation reaction. This *in-situ* synthesis yields an adduct that is the actual enzyme inhibitor. The adduct is deeply buried in the active site tunnel of ChAT and interactions with a hydrophobic pocket near the choline binding site have major implications for the molecular recognition of inhibitors. Our findings clarify the inhibition mechanism of AVPs, establish a drug modality that exploits a target-catalysed reaction between exogenous and endogenous precursors, and provide new directions for the development of ChAT inhibitors with improved potency and bioactivity.

Introduction

Choline acetyltransferase (ChAT) is a ubiquitous enzyme in the animal kingdom and the central upstream actor in acetylcholine (ACh) metabolism in cholinergic neurons[1], T-cells[2], and B-cells[3]. Alterations in ChAT expression or activity have been linked to conditions including Alzheimer's disease[4], schizophrenia[5], congenital myasthenic syndromes (CMS)[1], and chronic viral infections[6]. ChAT is also a potential target for pharmacotherapy for a range of medical conditions, including blood pressure disorders[7] and cholinergic overstimulation caused by organophosphorus nerve agents[8]; however, validation of ChAT´s utility as a drug target has not been possible due to the lack of useful inhibitors. Arylvinylpyridiniums (AVPs, *e.g.* the prototypical compound **1**, Figure 1) are the most widely studied ChAT inhibitors, with reported half maximal inhibitory concentrations (IC_{50}) in the low micromolar range[9]. While AVPs are reasonably potent *in vitro*, their confounding pharmacological profile[10,11], their propensity to photoisomerize[12], their electrophilic scaffold, and their permanent charge limits their usefulness in many applications. Furthermore, the mechanism of ChAT inhibition by AVPs is hitherto unknown[13–15], and the structure-activity relationships (SAR) of these compounds have yielded few clues as to how they could be improved[16]. In addition to AVPs, aryl-3-oxopropanaminium compounds (e.g *alfa*-NETA) are known inhibitors of ChAT [17] and a recent work by Darreh-Shori and co-workers have identified commercially avalible compounds by virtual screening that show inhibitory activity in *in vitro* assays[18,19].

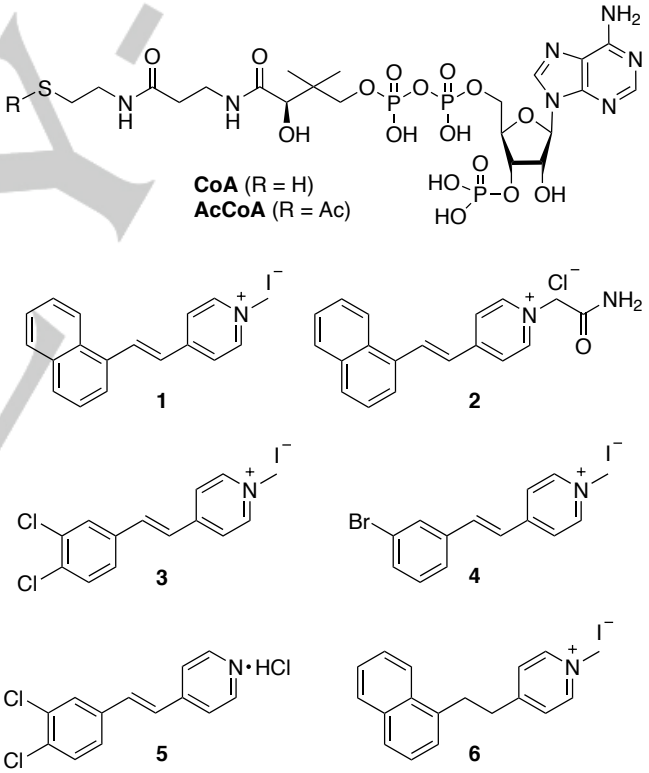

Figure 1. Ligands of ChAT. Chemical structures of compounds used in this study.

ChAT catalyses the synthesis of ACh from choline, using acetylcoenzyme A (**AcCoA**, Figure 1) as the acyl donor. Crystal structures of the apo- and holoenzyme show that ChAT has binding and catalytic domains within a narrow active site tunnel that extends through the enzyme (Figure 2)[20]. The choline and **AcCoA** binding sites are located on opposite sides of the tunnel. The choline hydroxyl group is activated by His324 and subsequently attacks the carbonyl carbon of the AcCoA thioester[20]. **AcCoA** and **CoA** have similar affinity for ChAT and in the absence of choline, ChAT catalyses the rapid hydrolysis of **AcCoA** to **CoA**[20].

10.1002/anie.202011989

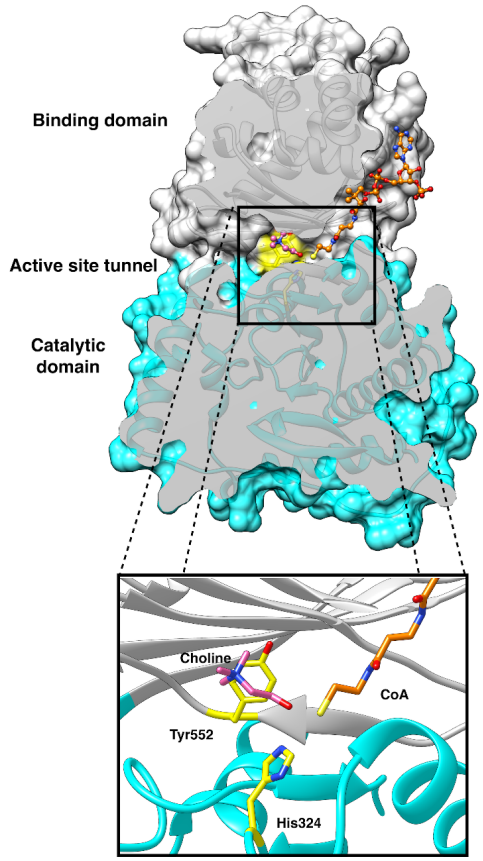

Figure 2. Molecular architecture of ChAT. Molecular architecture of ChAT with choline (pink) and **CoA** (orange) shown using stick representations. The active site His324 and the choline-binding Tyr552 are shown in yellow. The catalytic domain is shown in cyan and the binding domain is shown in grey. The figure was generated by a superposition of pdb entry codes 2FY3 and 2FY4.

Results and Discussion

To understand the molecular recognition of AVPs by ChAT, and the binding mode of this compound class, we determined the crystal structure of *Homo sapiens* ChAT modified with surface entropy reducing mutations (ChAT-SERM)[21] in complex with **1** and **CoA** (Supporting Information Table S1). The resulting 2.3 Å resolution X-ray crystal structure revealed the presence of a covalent bond between the thiol of **CoA** and the β-carbon of the vinyl linker of **1**, suggesting that a hydrothiolation reaction had occurred in close proximity to the catalytic His324 of ChAT, forming the adduct **1-CoA** (Figure 3 A, B). The pyridinium and naphthyl rings are not coplanar, indicating that **1-CoA** has a saturated linker (Figure 3A), consistent with a Michael-type addition facilitated by the electron-withdrawing pyridinium ring. The conformation of the His324 sidechain differs from that in the apo- and holoenzyme[20], and the structure suggests that the imidazole activates the thiol of **CoA** towards nucleophilic attack on the alkene moiety of **1**. Accordingly, the site of His324-assisted activation in the enzymatic synthesis of **1-CoA** differs from that in the natural reaction of ChAT, where the imidazole instead activates choline. The *in situ* assembled ligand exhibits excellent shape complementarity towards the interfacial active-site tunnel formed between the binding and catalytic domains of ChAT. Over 160 different AVPs and some analogous compounds with inhibitory activity against ChAT have been reported[9,22–27], but no structural information about their interaction with ChAT is available. Our crystal structure shows that **1-CoA** spans the choline and **AcCoA** binding sites of ChAT, with the electron-deficient pyridinium ring of **1-CoA** forming an edge-to-face interaction with the arene of Tyr552 and additional contacts to His324, Tyr436 and Ser438 (Figure 3 A). The naphthyl moiety of **1-CoA** is accommodated in a hydrophobic pocket with contacts to residues Pro98, Cys322, Leu332, Val542, Cys550, Tyr552, and Cys563 (Figure 3 B). The **CoA** moiety binds in a pose closely resembling that observed for the ChAT holoenzyme[20]. While the use of ChAT-SERM was necessary for these structural studies, subsequent experiments were performed using the 69 kDa R form of wild-type ChAT.

To verify that the hydrothiolation reaction observed in the crystal structure also occurred in solution, we studied the reaction using Ultra High Performance Liquid Chromatography - High Resolution Mass Spectrometry (UHPLC-HRMS). A reaction mixture containing ChAT, **1**, and **CoA** was filtered using a 10 kDa cut off filter to remove the protein fraction, and analysis of the supernatant showed the presence of **1-CoA** in the solution (Figure 4, Supporting Information Figure S1). Importantly, no reaction product was detected in a control sample without enzyme, confirming that the reaction is catalysed by ChAT. Enzyme catalysed hydrothiolation is known to occur in natural product biosynthesis[30], but to the best of our knowledge, this is the first observation of such a reaction *in vitro*.

To confirm the structure of the inhibitor adduct suggested by X-ray crystallography and UHPLC-HRMS, we prepared **1-CoA** as a mixture of diastereomers by organic synthesis. The reaction between **CoA**•3 Li and **1** progressed slowly at room temperature and required no catalyst or base when performed in dimethylformamide. A more practical reaction rate was achieved by using an excess of **CoA** at 40 °C. The only detectable side product formed under these conditions was the disulfide-linked **CoA**-**CoA** homodimer. The non-enzymatic synthesis of **1-CoA** is an unusual example of a Michael-type hydrothiolation that proceeds at mild conditions and involves a highly functionalised substrate. The HRMS spectrum of the product was identical to that of **1-CoA** produced in the ChAT-catalysed reaction, and the structure was further confirmed by a full Nuclear Magnetic Resonance (NMR) characterization (Supporting Information Materials and Methods).

Michael adducts that are formed reversibly may undergo retro-reaction, resulting in an equilibrium between reactants and product. By using NMR to assess the stability of **1-CoA** in phosphate buffered saline (PBS) at pH 7.4, we found that an equilibrium molar ratio of 9:1:1 between **1-CoA**, **1,** and **CoA** was rapidly reached upon dissolution (Supporting Information Figure S2 A, B). The stability of the adduct in aqueous buffer was further corroborated by UHPLC-HRMS, which showed that the concentration of **1-CoA** in ammonium acetate buffer (pH 6.8) was constant during 7 hours at 10 °C (Supporting Information Figure S2 C). Although the specific experimental conditions may influence the Michael - retro - Michael equilibrium and thereby determine the effective concentrations of **1-CoA**, **1** and **CoA**, these experiments show that the inhibitor adduct was sufficiently stable in aqueous buffer for further experiments.

To determine whether the *in situ* formation of **CoA**-adducts is a common inhibitory mechanism for all AVPs, we reviewed the chemical structures of previously reported compounds in this class[9,22–27], and found that all active compounds possess a Michael-acceptor moiety (*i.e.* a vinyl linker and an electron-withdrawing heteroarene) and could therefore all be hydrothiolation substrates. To test this hypothesis, we studied the reaction in solution using ChAT, **CoA** and a representative subset of AVPs (**2**-**5**, Figure 1). In all cases, the expected hydrothiolation product (*i.e.* **2**-**5**-**CoA**) was observed by UHPLC-HRMS (Supporting Information Table S2). Conversely, no reaction product was observed for the negative control **6** (Figure 1), which lacks the Michael acceptor motif. A Principal Component Analysis[31] (PCA, Supporting Information Figure S3) of parameters describing molecular size, electronic properties and lipophilicity shows that the chosen subset is representative of

10.1002/anie.202011989

active AVPs (*i.e.* reported apparent half maximal inhibition concentration IC_{50} lower than 15 μM**)**. We therefore suggest that *in-situ* assembly of **CoA**-adducts is a common inhibition mechanism for all AVP inhibitors. We also synthesised the aryl-3-oxopropanaminium compound α-NETA[17]. In our hands, this compound was not sufficiently stable to allow structural or biochemical characterisation of its interaction with the enzyme.

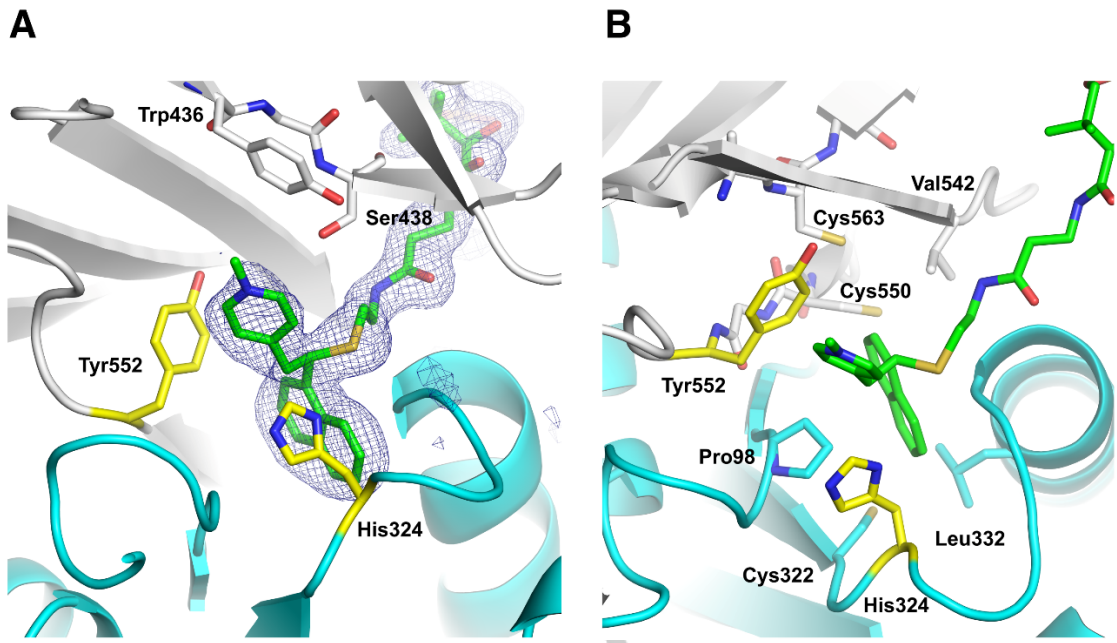

Figure 3. ChAT catalyses a hydrothiolation reaction between 1 and CoA. A) X-ray crystal structure of the hydrothiolation reaction product **1-CoA** (green) in complex with ChAT-SERM with the catalytic and binding domains shown in cyan and grey respectively. The Polder omit map is shown at a contour level of 4 sigma (blue). B) The naphthyl moiety of **1-CoA** is accommodated in a hydrophobic pocket.

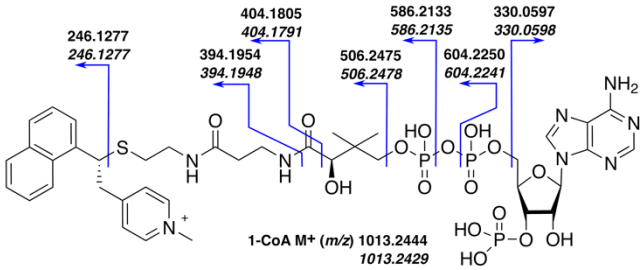

Figure 4. Confirmation of the chemical structure of 1-CoA by HRMS. The fragmentation of the product formed in the reaction between **1** (40 μM) and **CoA** (80 μM) catalysed by ChAT (4.6 μM) in HRMS analysis. Measured (bold) and theoretical (bold italic) high resolution masses of fragments are indicated.

Ligand-induced shifts in the midpoint of a protein's melting temperature (T_m) correlate with the protein's affinity for the ligands in question[32]. We therefore used Circular Dichroism (CD) spectroscopy to investigate the individual contributions of the reactants and the *in situ* formed **CoA** adducts to the temperature stability of ChAT. Compounds **1**-**6** had no effect on the T_m of ChAT, but binding of **CoA** increased the T_m by approximately 3 °C (Table 1, Supporting Information Figure S4). When both **1**-**5** and **CoA** were present, the T_m increased even further by up to 12 °C. For comparative purposes, compound **6** (which can presumably occupy the same binding site as **1**-**5** but lacks the Michael acceptor motif) did not shift the T_m, even in the presence of **CoA**. These results show that **1**-**5**-**CoA** stabilize the folded state of the enzyme considerably and that this effect is due to the formed adducts and not to the binding of the individual components of the reaction. Furthermore, the naphthyl containing inhibitors **1**,**2-CoA** provide a higher degree of stabilization than adducts that have a substituted phenyl moiety (**3**-**5-CoA**). Interestingly, we see only minor differences between the charged *N*-methylpyridinium **3-CoA** and the pyridine derivative **5-CoA**, indicating that interaction with Tyr552 only marginally contribute to their stabilization of ChAT.

Assays used for measuring the inhibitory potency of AVPs include **CoA** or **AcCoA**[28,33,34], which is rapidly hydrolysed to **CoA**[20]**,** and do not account for the fact that AVPs and **CoA** are co-substrates in the enzyme-catalysed hydrothiolation reaction. The propensity for inhibitor adduct decomposition by retro-Michael reaction for a given compound may also give confounding results when determining the inhibitory potency. It is therefore unsurprising that the SAR of AVPs remains poorly understood, and that that there has been no development of improved inhibitors based on the AVP scaffold. The chemically prepared **1-CoA** offers the opportunity to circumvent these problems by studying a pre-assembled ChAT inhibitor.

The association kinetics was studied by following the time-dependent decline in the enzymatic activity at various concentrations of chemically prepared **1-CoA.** Under the assay conditions, where choline, **CoA** and **1-CoA** compete for the same binding sites, we found that the inhibition is slow and occurs on a time scale of minutes, even at inhibitor concentrations as high as 100 μM (Figure 5). For comparative purposes, the Michaelis constants (K_M) are 11.9 and 8.8 μM for **AcCoA** and **CoA**, respectively[35].

Table 1. Thermal stabilization of ChAT by inhibitor adducts and their target residence time.

Compound[a]	T_m (°C)[b]		k_{off} (min^{-1})[c]	τ (min)[c]
	- CoA	**+ CoA**	**+ CoA**	
-	49.2 (48.0 - 50.4)	52.4 (51.9 - 52.9)	-	
1	48.3 (45.8 - 50.8)	63.8 (62.2 - 65.4)	0.080 (0.077 - 0.083)	12.5
2	49.4 (48.6 - 50.3)	64.5 (62.0 – 66.9)	0.097 (0.093 - 0.102)	10.3
3	50.0 (49.2 - 50.9)	59.0 (57.0 - 61.0)	0.342 (0.317 - 0.371)	2.9
4	49.2 (46.9 - 51.5)	57.5 (54.9 - 60.0)	0.135 (0.129 - 0.141)	7.4
5	48.9 (47.4 - 50.4)	57.3 (55.0 - 59.6)	0.156 (0.148 - 0.164)	6.4
6	49.6 (48.5 - 50.7)	52.5 (49.7 - 55.3)	-	
Choline	48.8 (46.6 – 51.2)	52.7 (51.0 – 53.9)	-	

[a]All samples contained ChAT
[b]Determined by temperature scanning CD experiments, mean, *n*=3-4, (95% CI)
[c]Determined by jump dilution experiments, mean, *n*=3 independent experiments, each measured in quadruplicates, (95% CI)

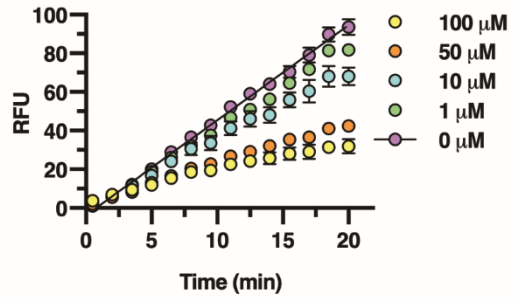

Figure 5. The inhibition kinetics of 1-CoA. The inhibition progress curve at various concentrations of chemically prepared **1-CoA**. The enzymatic activity was determined using a fluorescence assay and the reaction mixture also contained **CoA** (9.3 μM) and acetylthiocholine (9.5 mM). The data (n=3, mean and SD plotted) was baseline corrected and the solid line represents the fit of the experimental data of the control sample to a linear regression line (R^2=0.984).

The thermodynamics of binding was characterized by isothermal calorimetry (ITC). The Gibbs free energy of binding ($\Delta G°$) of **1-CoA** was mainly governed by entropic contributions ($-T\Delta S°$), while the binding of **CoA** was dominated by enthalpic terms ($\Delta H°$) (Figure 6 A, Supporting Information Figure S4). Both ligands have dissociation constants in the high nanomolar range K_d (**1-CoA**) = 8.9×10^{-7} M (95% CI 1.3×10^{-7} – 1.8×10^{-6}) and K_d (**CoA**) = 8.5×10^{-7} M (95% CI 8.1×10^{-7} – 8.9×10^{-7}). A comparison of the crystal structure of ChAT-SERM in complex with **CoA** (pdb entry code 2FY4) and the complex between **1-CoA** and ChAT-SERM reveals that several water molecules are displaced from a hydrophobic pocket by the naphthyl moiety of **1-CoA**, likely contributing to the difference in thermodynamic profile (Figure 6 B).

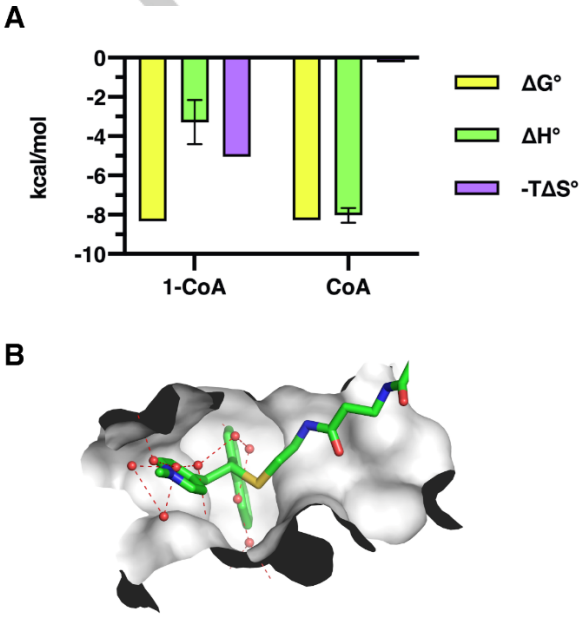

Figure 6. The thermodynamics of 1-CoA. (A) The thermodynamic parameters of **1-CoA** and **CoA** (n=3-4, mean and 95% CI are plotted, the isotherms are shown in Extended Data Figure 5). B) Water displacement upon **1-CoA** binding to ChAT. The binding of **1-CoA** displaces water molecules from the arene-binding hydrophobic pocket and the choline binding site. The figure was generated by a superpositioning of the crystal structure of the complex between ChAT-SERM and **CoA** (pdb entry code 2FY4) and the crystal structure of the complex between **1-CoA** and ChAT-SERM. Water molecules that are sterically incompatible with the AVP moiety of 1-CoA are shown as red spheres. Potential hydrogen bonds are shown as dashed lines, **1-CoA** is shown in green and the active site tunnel is shown as a surface representation.

We next investigated the pre-steady-state kinetics of the *in situ* assembly of **1-CoA** by pre-incubating ChAT with **CoA** to generate **CoA**•ChAT. The reaction was initiated by adding **1,** and following termination, UHPLC-HRMS was used to quantify the production of **1-CoA**. The process was too fast to be resolved at 25 °C by discontinuous sampling, so the experiments were conducted at 0 °C. We found that the *in-situ* hydrothiolation reaction exhibited a distinct burst phase during the first 20 minutes (Figure 7). A second burst was observed upon adding a second equivalent of ChAT *apo* enzyme after 25 min. Both burst phases could be fitted to the same pseudo-first order association kinetics model. We determined the rate constant for the pre-steady-state phase (k_{pss}) to be 0.05 min^{-1} (95% CI 0.034 - 0.080) and the doubling time of **1-CoA** synthesis to be 12.8 min (95% CI 8.68 - 20.12). The rate constant during the steady state (k_{ss}, *i.e.* 55-105 min) was reduced tenfold, to 0.005 min^{-1} (95% CI 0.0018x - 0.0091). Taken together, these results show that the hydrothiolation reaction is fast and that it is the association of **1** to ChAT that limits the rate of production of **1-CoA** during the pre-steady-state phase. The rate of **1-CoA** assembly is reduced due to product inhibition once a steady state is established.

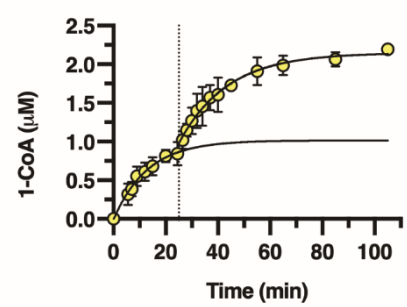

Figure 7. The kinetics of *in situ* hydrothiolation. Kinetic analysis of **1-CoA** formation. The reaction was initiated by adding **1** (40 μM) to ChAT (0.9 μM) preloaded with **CoA** (80 μM) at 0 °C. A second equivalent of ChAT apo enzyme was added at 25 min (n = 3, mean and SD plotted, data fitted to a pseudo-first order association kinetics model, R^2 = 0.884 and R^2 = 0.877 for the 0-25 min, and 25-105 min periods, respectively).

To investigate the dissociation kinetics of *in situ* assembled inhibitor adducts, we performed jump-dilution experiments in which the reactants were mixed, incubated, and then diluted 4200-fold. The dissociation of the adduct was followed by continuously monitoring the enzymatic activity. We found that the dilution restored the catalytic activity of ChAT in a time-dependent manner (Figure 8 A). Furthermore, a non-linear phase was observed for samples containing *in situ* assembled **1-5-CoA** due to a slow dissociation of the adducts from ChAT. We determined the first order rate constant for dissociation (k_{off}) and found that the target residence time (τ) varies between 2.9 and 12.5 minutes (Table 1). As a reference, the catalytic turnover (k_{cat}) of the natural reaction is 99.6 s^{-1} [1], showing that the exit of **1-5-CoA** is several orders of magnitude slower than the exit of **CoA**. We also note that inhibitors that have a naphthyl moiety (**1**,**2-CoA**) have a slower dissociation and a longer target residence time than adducts with a substituted phenyl moiety (**3-5-CoA**, Table 1).

Entry of chemically prepared **1-CoA** into the active site tunnel of ChAT shown by the inhibition progress curves (Figure 5), as well as the reversibility of binding of *in situ* assembled inhibitor adducts shown by the jump dilute experiments (Figure 8 A) is unexpected since the X-ray crystal structure shows that the tunnel is constricted by an α-helix (residue 329-342) and two β-sheets (residue 435-440 and 537-542, Figure 8 B) that form a clamp around the propanamido linker of **CoA**. This suggests that dynamics, likely involving a significant structural rearrangement or domain movement of ChAT may be involved in the trafficking of **1-CoA**.

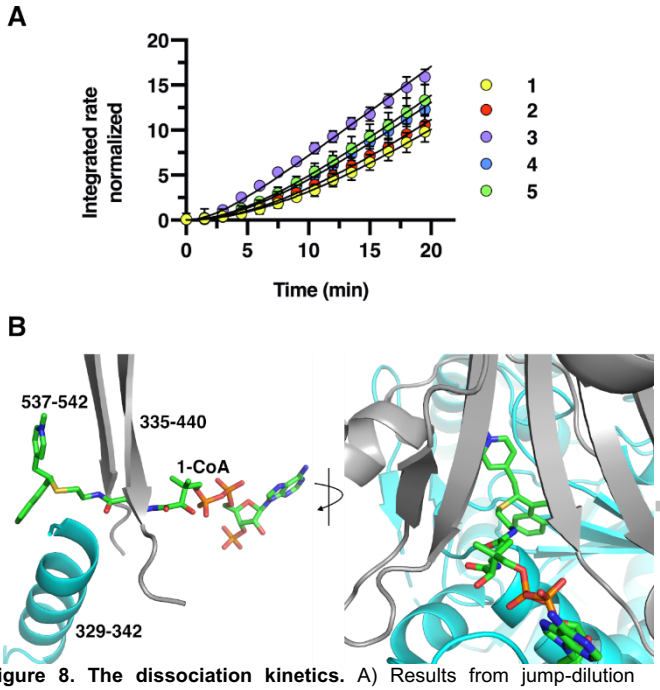

Figure 8. The dissociation kinetics. A) Results from jump-dilution experiments in which ChAT (2.7 μM), **CoA** (80 μM) and **1**, **2**, **3**, **4** or **5** (100 μM) were mixed, incubated, and then diluted 4200-fold. Enzymatic activity was determined using a fluorescence assay (n=3 independent reactions each measured in quadruplicates, mean and SD plotted). The solid lines represent fits of experimental data to the integrated rate equation (1) from which the dissociation constants (k_{off}) are determined. (B) The narrow binding site of **1-CoA**. The X-ray crystal structure shows that **1-CoA** binds through a constriction of the active site tunnel formed by two β-sheets and one α-helix.

Conclusion

We have shown that **1** and **CoA** are substrates of a ChAT-catalysed hydrothiolation reaction, and that the inhibition of ChAT attributed to **1** is actually due to the *in situ* synthesis of the adduct **1-CoA**. This mechanism is common to a representative subset of AVPs (**1-5**), suggesting that it is the main mechanism of ChAT inhibition for this compound class and that *thia*-Michael acceptor ability is a crucial component of the SAR of AVPs. Our results show that the bioactive forms of AVPs are their adducts with **CoA**, which thus constitute a new class of ChAT inhibitors. Given these new insights into the mechanism of ChAT inhibition by AVPs and the reversibility of adduct formation, we advocate a reassessment of previous studies on AVPs. Our kinetic data show that the association of chemically prepared **1-CoA** as well as the dissociation of *in situ* assembled **1-5-CoA** is slow and may involve a structural reorganisation of ChAT. The slow trafficking may provide an opportunity to develop non-reactive, tunnel spanning inhibitors with prolonged target residence time. The X-ray crystal structure of **1-CoA** in complex with ChAT-SERM establishes the binding mode of a tunnel-spanning inhibitor and provides a template for such development efforts. Analysis of the dissociation kinetics, shifts in thermal stabilization, thermodynamics and the X-ray crystal structure show that interactions between the arene of the AVPs and a hydrophobic pocket near the choline binding Tyr552 play an important role in the molecular recognition of AVP-CoA adducts and is a significant determinant of inhibitor potency. In conclusion, our results establish the mechanism of ChAT inhibition by AVPs, provide directions for the development of non-reactive ChAT inhibitors and illustrate a novel drug modality concept based on *in situ* inhibitor assembly from an exogenous precursor and an endogenously produced co-substrate.

Acknowledgements

We thank Dr. Brian Shilton for helpful comments and discussions during this work. We are also grateful to the staff at ESRF beamline ID23-2, David C. Andersson for help with the CD measurements, and Kristoffer Brännström at the Biochemical Imaging Centre at Umeå University for assistance with the ITC measurements.
Funding We thank Swedish Ministry of Defence, the Knut and Alice Wallenberg foundation program NMR for life, SciLifeLab. NH is funded by the Industrial Doctoral School for Research and Innovation at Umeå University and by the Swedish Defence Research Agency (FOI).

Competing interests The authors declare no competing interests.

Data and material availability: The coordinate file is available at rcsb.org with accession number 7AMD.

Keywords: Choline acetyltransferase; in situ assembly; hydrothiolation, Coenzyme A, Drug discovery

[1] K. Ohno, A. Tsujino, J. M. Brengman, C. M. Harper, Z. Bajzer, B. Udd, R. Beyring, S. Robb, F. J. Kirkham, A. G. Engel, *Proc. Natl. Acad. Sci. U. S. A.* **2001**, *98*, 2017–2022.

[2] M. Rosas-Ballina, P. S. Olofsson, M. Ochani, S. I. Valdés-Ferrer, Y. A. Levine, C. Reardon, M. W. Tusche, V. A. Pavlov, U. Andersson, S. Chavan, T. W. Mak, K. J. Tracey, *Science (80-.).* **2011**, DOI 10.1126/science.1209985.

[3] C. Reardon, G. S. Duncan, A. Brüstle, D. Brenner, M. W. Tusche, P. Olofsson, M. Rosas-Ballina, K. J. Tracey, T. W. Mak, *Proc. Natl. Acad. Sci. U. S. A.* **2013**, DOI 10.1073/pnas.1221655110.

[4] T. D. Bird, S. Stranahan, S. M. Sumi, M. Raskind, *Ann. Neurol.* **1983**, *14*, 284–293.

[5] C. N. Karson, M. F. Casanova, J. E. Kleinman, W. S. T. Griffin, *Am. J. Psychiatry* **1993**, *150*, 454–459.

[6] M. A. Cox, G. S. Duncan, G. H. Y. Lin, B. E. Steinberg, L. X. Yu, D. Brenner, L. N. Buckler, A. J. Elia, A. C. Wakeham, B. Nieman, C. Dominguez-Brauer, A. R. Elford, K. T. Gill, S. P. Kubli, J. Haight, T. Berger, P. S. Ohashi, K. J. Tracey, P. S. Olofsson, T. W. Mak, *Science (80-.).* **2019**, *363*, 639–644.

[7] P. S. Olofsson, B. E. Steinberg, R. Sobbi, M. A. Cox, M. N. Ahmed, M. Oswald, F. Szekeres, W. M. Hanes, A. Introini, S. F. Liu, N. E. Holodick, T. L. Rothstein, C. Lövdahl, S. S. Chavan, H. Yang, V. A. Pavlov, K. Broliden, U. Andersson, B. Diamond, E. J. Miller, A. Arner, P. K. Gregersen, P. H. Backx, T. W. Mak, K. J. Tracey, *Nat. Biotechnol.* **2016**, *34*, 1066–1071.

[8] A. P. Gray, R. D. Platz, T. C. P. Chang, T. R. Henderson, K. Takahashi, K. L. Dretchen, *J. Med. Chem.* **1988**, *31*, 807–814.

[9] J. C. Smith, C. J. Cavallito, F. F. Foldes, *Biochem. Pharmacol.* **1967**, *16*, 2438–2441.

[10] S. -M Aquilonius, L. Frankenberg, K. -E Stensiö, B. Winbladh, *Acta Pharmacol. Toxicol. (Copenh).* **1971**, *30*, 129–140.

[11] B. A. Hemsworth, F. F. Foldes, *Eur. J. Pharmacol.* **1970**, *11*, 187–194.

[12] H. L. White, C. J. Cavallito, *BBA - Enzymol.* **1970**, *206*, 242–251.

[13] H. L. White, C. J. Cavallito, *Biochim. Biophys. Acta - Enzymol.* **1970**, *206*, 343–358.

[14] B. R. Baker, R. E. Gibson, *J. Med. Chem.* **1972**, *15*, 639–642.

[15] A. Y. Chweh, J. F. DeBernardis, J. F. Siuda, N. G. Rondan, J. E. Abola, D. J. Abraham, *J. Med. Chem.* **1984**, *27*, 825–830.

[16] V. Chandrasekaran, G. B. McGaughey, C. J. Cavallito, J. P. Bowen, *J. Mol. Graph. Model.* **2004**, *23*, 69–76.

[17] B. V. R. Sastry, N. Jaiswal, L. K. Owens, V. E. Janson, R. D. Moore, *J. Pharmacol. Exp. Ther.* **1988**.

[18] R. Kumar, A. Kumar, B. Långström, T. Darreh-Shori, *Sci. Rep.* **2017**, DOI 10.1038/s41598-017-16033-w.

[19] R. Kumar, A. Kumar, A. Nordberg, B. Långström, T. Darreh-Shori, *Alzheimer's Dement.* **2020**, DOI 10.1002/alz.12113.

[20] A. R. Kim, R. J. Rylett, B. H. Shilton, *Biochemistry* **2006**, *49*, 14621–14631.

[21] A. R. Kim, T. Dobransky, R. J. Rylett, B. H. Shilton, *Acta Crystallogr. Sect. D Biol. Crystallogr.* **2005**, *61*, 1306–1310.

[22] C. J. Cavallito, H. S. Yun, T. Kaplan, J. C. Smith, F. F. Foldes, *J. Med. Chem.* **1970**, *13*, 221–224.

[23] B. R. Baker, R. E. Gibson, *J. Med. Chem.* **1971**, *14*, 315–322.

[24] R. L. Ryan, W. O. McClure, *Neurochem. Res.* **1981**, *6*, 163–173.

[25] N. B. Mehta, D. L. Musso, H. L. White, *Eur. J. Med. Chem.* **1985**, *20*, 443–446.

[26] J. F. DeBernardis, P. Gifford, M. Rizk, R. Ertel, D. J. Abraham, J. F. Siuda, *J. Med. Chem.* **1988**, *31*, 117–121.

[27] E. Alcalde, T. Roca, A. Barat, G. Ramirez, P. Goya, A. Martinez, *Bioorganic Med. Chem. Lett.* **1992**, *12*, 1493–1496.

[28] C. J. Cavallito, H. S. Yun, J. Crispin Smith, F. F. Foldes, *J. Med. Chem.* **1969**, *12*, 134–138.

[29] C. J. Cavallito, H. S. Yun, M. L. Edwards, C. J. Cavallito, H. S. Yun, M. L. Edwards, F. F. Foldes, *J. Med. Chem.* **1971**, *14*, 130–133.

[30] K. L. Dunbar, D. H. Scharf, A. Litomska, C. Hertweck, *Chem. Rev.* **2017**, DOI 10.1021/acs.chemrev.6b00697.

[31] H. Abdi, L. J. Williams, *Wiley Interdiscip. Rev. Comput. Stat.* **2010**, DOI 10.1002/wics.101.

[32] M. W. Pantoliano, E. C. Petrella, J. D. Kwasnoski, V. S. Lobanov, J. Myslik, E. Graf, T. Carver, E. Asel, B. A. Springer, P. Lane, F. R. Salemme, *J. Biomol. Screen.* **2001**, *6*, 429–440.

[33] L. T. Potter, V. A. Glover, J. K. Saelens, *J. Biol. Chem.* **1968**, *243*, 3864–3870.

[34] R. Kumar, B. Långström, T. Darreh-Shori, *Sci. Rep.* **2016**, *6*, 31247.

[35] L. B. Hersh, B. Coe, L. Casey, *J. Neurochem.* **1978**, *30*, 1077–1085.

10.1002/anie.202011989

WILEY-VCH

RESEARCH ARTICLE

Entry for the Table of Contents

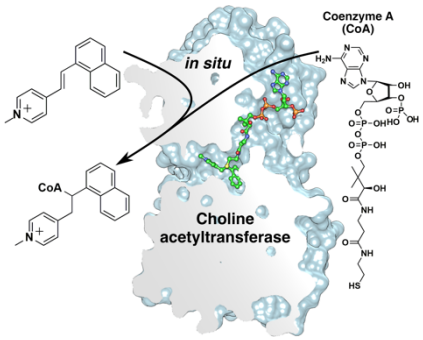

We show that arylvinylpyridiniums (AVPs), the most widely studied class of inhibitors of the potential drug target choline acetyltransferase (ChAT), act as substrate in an unusual coenzyme A-dependent hydrothiolation reaction. This *in-situ* synthesis yields an adduct that is the actual enzyme inhibitor. Our findings clarify the inhibition mechanism of AVPs and establish a drug modality that exploits a target-catalyzed reaction between exogenous and endogenous precursors.